



ACCEPTED MANUSCRIPT

This is an early electronic version of an as-received manuscript that has been accepted for publication in the Journal of the Serbian Chemical Society but has not yet been subjected to the editing process and publishing procedure applied by the JSCS Editorial Office.

Please cite this article Sushma, A. Keshav, and M. Ramachandran, *J. Serb. Chem. Soc.* (2024) <https://doi.org/10.2298/JSC240520084S>.

This “raw” version of the manuscript is being provided to the authors and readers for their technical service. It must be stressed that the manuscript still has to be subjected to copyediting, typesetting, English grammar and syntax corrections, professional editing and authors’ review of the galley proof before it is published in its final form. Please note that during these publishing processes, many errors may emerge which could affect the final content of the manuscript and all legal disclaimers applied according to the policies of the Journal.



J. Serb. Chem. Soc. **00(0)** 1-14 (2024)
JSCS-12983

Biosorptive removal of cobalt (II) ion from wastewater using pomegranate peel activated carbon as biosorbent

SUSHMA, AMIT KESHAV, MANIVANNAN RAMACHANDRAN*

Department of Chemical Engineering, National Institute of Technology Raipur, Chhattisgarh, India.

(Received 20 May; revised 13 June; accepted 27 September 2024)

Abstract: Cobalt is used to link the components during integrated circuits (ICs) fabrication. Cobalt ion is common in chemical mechanical planarization (CMP) spent slurry. The role of cobalt (Co) is indispensable in the semiconductor industry and its presence in the wastewater is inevitable. Cobalt metal ions are toxic heavy metals that can cause serious health issues such as heart disease, nausea, vision sterility, thyroid damage, bone defects, and diarrhea. The present work researches the potential application of *Punica granatum* (pomegranate) peel-activated carbon (PPAC) as an adsorbent for cobalt metal ion removal by adsorption. This work examines the influence of initial cobalt ion concentration, pH, contact duration, and adsorbent dose on the removal efficiency (RE) and adsorption capacity (AC) of Co^{2+} ions, and the results of the findings are discussed. The Co(II) adsorption kinetic study revealed that a pseudo-2nd-order is best fitted with a rate constant of $\sim 0.00358 \text{ g mg}^{-1} \text{ min}^{-1}$. The adsorbent utilized in this work was assessed using SEM, EDAX, FTIR, XRD, and TGA. EDX composition of post-adsorbent usage showed the presence of cobalt. Cobalt ion adsorption onto the PPAC was best fitted with the Freundlich isotherm model. Co(II) adsorption was found to be endothermic based on the thermodynamic characteristics evaluated for the carbon. At ambient temperature ($\sim 303 \text{ K}$) and neutral pH, PPAC was found to have a maximum AC of $\sim 85 \text{ mg/g}$ with a RE of $\sim 90 \%$.

Keywords: semiconductor; adsorption capacity; Freundlich; pseudo-second order; Langmuir.

INTRODUCTION

Cobalt, copper, nickel, zinc, and other heavy metal ions are frequently detected in waste effluent from mineral extraction, tanneries, as well as from the electronic, electroplating, and petrochemical sectors. Since heavy metals cannot be broken down by nature, they often accumulate in living organisms and can cause

* Corresponding author. E-mail: rmani.che@nitrr.ac.in
<https://doi.org/10.2298/JSC240520084S>

several illnesses.¹ Heavy metal ion concentration in wastewater is significantly greater than those advised by environmental regulations. Several techniques are being adapted to extract these metal ions from industrial effluents before disposal. The semiconductor industry uses cobalt as interconnect material in the manufacturing of integrated circuits (IC). However, during the chemical mechanical planarization of cobalt, the spent slurry might contain the cobalt ions, which are discarded as waste.^{2,3} The allowable cobalt concentrations in drinking water, inland surface water and irrigation water are 0.01, 0.05, and 1 mg/l respectively.^{4,5} A deficit in cobalt inhibits the production of new red blood cells, but excessive intake into the body can be extremely dangerous.⁶ Cobalt poisoning can result in blindness, deafness, and critical illness like heart failure.⁶ Environmentalists are deeply concerned with the efficient removal of heavy metals before their release into the environment due to toxicity even at low dosages.⁷

Various treatment methods have been employed, including ion exchange through the membrane, filtration, adsorption, chemical precipitation, and coagulation-flocculation to remove the cobalt metal ion. However, the adsorption process has been proven to be simpler, more advantageous, and more efficient than other methods.⁸ As agricultural wastes are inexpensive and do not pollute the environment, agro-based adsorbents are preferred to remove heavy metals from aqueous solutions.

Several adsorbents such as hazelnut¹, lemon peel⁹, orange peel⁶, black tea waste¹⁰, rice husk¹¹, and eucalyptus¹² - based activated carbon have been reported for the exclusion of cobalt ions from wastewater. However, pomegranate peel (PP) (*Punica granatum*) powder-based adsorbent has not been reported for the adsorption of cobalt yet. Pomegranate fruit is popular in both raw and processed forms and is consumed as juice, preserves, and wine. The pomegranate skin can make as much as 30 % of the fruit overall, yet it is frequently thrown out as a leftover waste. Gallic acid, ellagic acid, flavone derivatives, and hydroxycinnamic acids are present in PP.¹³ PP contains lignocellulosic waste and as a result, there has been an increase in research on valorization of this waste in recent years.¹⁴ Recently, adsorbents such as polypyrrole-modified carbon nanotubes¹⁵ and Ca(OH)₂ modified quartz rock particles¹⁶ were utilized to remove the cobalt metal ion from the wastewater. Those reported adsorbents were relatively expensive when compared with the proposed adsorbent. Nowadays, fruit peels are transformed into biosorbents to remove harmful pollutants, which would increase the economic worth of these inexpensive biowastes. The current study explores the possibility of using PP-activated carbon as an adsorbent to eliminate the cobalt metal ions from the simulated semiconductor wastewater.

EXPERIMENTAL

Chemicals

Analytical-grade chemicals were used in this work. Cobalt (II) sulphate heptahydrate ($\text{CoSO}_4 \cdot 7\text{H}_2\text{O}$), hydrochloric acid (HCl), and potassium hydroxide (KOH) were procured from LOBA CHEMIE Pvt. Ltd in India. Cobalt sulphate solution pH was maintained using HCl or KOH, $\text{CoSO}_4 \cdot 7\text{H}_2\text{O}$ was used for the preparation of metal ion solution.

PP-activated carbon preparation

PP was gathered from the fruit market in Raipur, Chhattisgarh. Before the treatment, PPs were cleaned using DIW and dehydrated the peel in a hot air oven at 80°C for 48 h. The dehydrated peels were finely powdered with the help of a mixer grinder and sieved through 355-micron mesh. PP dried powder was thermally activated at 300°C for 30 min. Eventually, the powder was washed with 0.1 N HCl solution several times until the pH reached 7. Finally, the thermally triggered carbon powder was dehydrated in a hot air oven for 30 min at 70°C .

Characterization

The surface morphology of PP, PP-activated carbon (PPAC) (pre-adsorption), and PPAC post-adsorption of Co (PPACC) were analyzed with ZEISS EVO-18 model scanning electron microscopy (SEM). Oxford, INCA 250 model EDS was deployed for the elemental analysis. Bruker alpha model FTIR was employed to reveal the surface functional group of PP, PPAC, and PPACC and the surface area was examined using a Smart Sorb 92/93 model Brunauer-Emmett-Teller (BET) analyzer. Hitachi Nexta HTA 300 TGA was employed to understand the thermal performance of the adsorbent. The crystalline nature of the sample was determined using XRD of PAN Analytical 3kW X'pert, which emits Cu-K α radiation source ($\lambda=0.015418$ Å/nm) with 2θ in the range between 20 and 90° ($3.5^\circ/\text{min}$ scan rate). The point of zero charge (PZC) experimental procedure reported in the literature was adapted in this work.⁶ Thermally activated PP powder was used in this study.

Batch adsorption

Unless mentioned otherwise, all the adsorption batch experiments were executed at 25°C , with 0.5 g adsorbent dosage in 100 ml metal ion solution of 500 ppm at pH 7 for 90 min contact duration. The effect of initial concentration (10 - 1000 ppm), pH (2 - 11), adsorbent dose (0.1 - 1 g), and contact time (15 - 150 min) on the AC and RE were studied. Metal ion solution with adsorbent was kept in a shaker for 90 min at a rate of 300 rpm. After filtration of the sample, the amount of the cobalt ion in the filtrate was measured using atomic absorption spectroscopy (AAS) of ECIL AAS4141 at 241 nm wavelength. All the trials were performed in triplicate, and the average AC was stated with the standard deviation. The equation used for the calculation of AC and RE is presented in Eq. S-1 and S-2 (Supplementary Material).

RESULTS AND DISCUSSION

Characterization

TGA / DSC / DTA analysis

The thermal response of PP powder was explored employing differential thermogravimetry (DTG), differential scanning calorimetry (DSC), and thermogravimetry (TG) analyses in an N_2 environment from atmospheric temperature to 1000°C with a warming rate of $10^\circ\text{C}/\text{min}$, and the findings are presented in Fig. 1a. TG outcome reveals that the powder underwent significant

weight loss in the first 500 °C and remains almost constant thereafter. The initial stage of weight loss of ~8.6 % (i.e., up to 100 °C) is ascribed to the exclusion of moisture content, while the later phase of weight loss of ~60.4 % is owing to the breakdown of hemicellulose, and lignin.¹⁷ The DSC peak shows that the thermal decomposition of hemicellulose, and lignin in PP powder is an exothermic process.

FTIR analysis

Fig. 1b illustrates the FTIR spectra of PP, PPAC, and PPACC used in this study. Cobalt ions adhere to the adsorbent surface through the active sites. Chemical functional groups *viz.*, amine, hydroxyl, carbonyl, and amide group are liable for the adsorption. FTIR spectra of PP show a robust peak at 677 cm^{-1} , 944 cm^{-1} , 1523 cm^{-1} , 2326 cm^{-1} , and 3733 cm^{-1} that represents the O-H stretching of the phenolic group¹⁸, symmetrical stretching of N-C=O group¹⁹, symmetric stretch of -COO group²⁰, O=C=O stretching of the carbon dioxide group²¹, and OH group²² respectively. However, those peaks disappear in the PPAC sample due to the thermal treatment of PP. But there exist two peaks, *viz.*, 1706 cm^{-1} and 2928 cm^{-1} corresponding to the ketonic group²³ and -C-H of CH_2 (asymmetrical stretching) group²⁴ respectively in the PPAC sample which is responsible for the cobalt metal ion adsorption. Those peaks get suppressed in the PPACC sample due to the adsorption of the cobalt metal ion. A new peak at 2353 cm^{-1} ascribed to C-O of carboxylic acids, alcohols, esters, and ethers is formed for the PPACC sample.²⁵

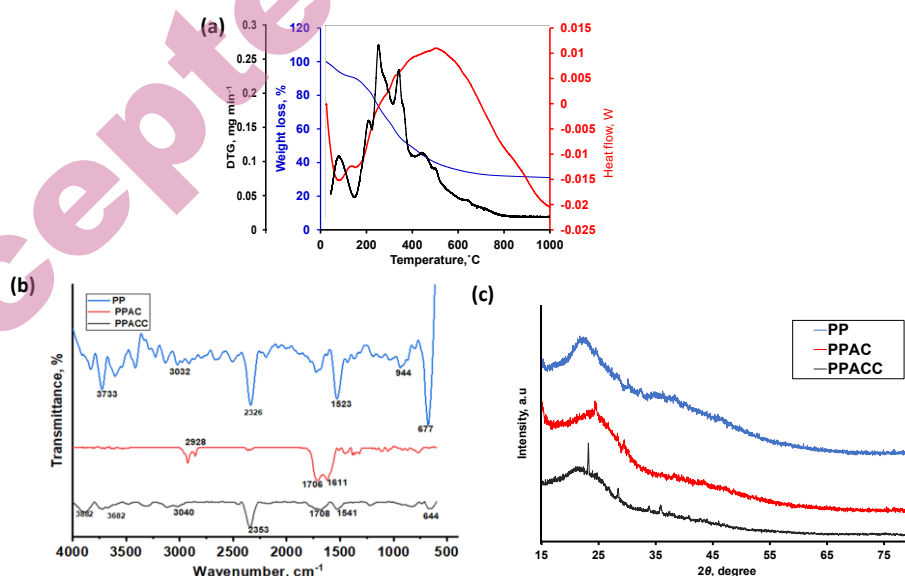


Fig. 1. (a) TGA, DSC, and DTG curve of PP (b) FTIR spectra of PP, PPAC, and PPACC (c) X-ray diffraction spectra of PP, PPAC, and PPACC.

XRD analysis

Fig. 1c shows the XRD spectra of PP, PPAC, and PPACC. PP showed a broad peak at near 25° with lower intensity. However, the same peak becomes relatively less broad (*i.e.*, sharper) and slightly shifted toward the lower diffraction angle for the PPACC sample. All the XRD spectrum reveals the presence of non-cellulosic *viz.*, hemicellulose and lignin in the PP and the absence of sharp diffraction peaks of crystalline cellulosic material.¹⁷ PPACC samples showed peaks of cobalt sulfate, which matches well with the reported literature.²⁶

BET surface area

The AC is found to escalate with a rise in the surface area, which plays a crucial role. PP, PPAC, and PPACC samples were used to evaluate the surface area. PP sample claimed the least surface area of $0.298 \text{ m}^2 \text{ g}^{-1}$, while PPAC exhibited $4.056 \text{ m}^2 \text{ g}^{-1}$. The thermal activation method has increased almost 15 times the surface area when compared with the adsorbent before activation.^{27,28}

SEM and EDX

The surface morphology and the elemental composition of PP, PPAC, and PPACC samples were probed using SEM and EDX respectively and the images and composition are presented in Fig. 2(a-c). Literature suggests that the PP sample contains lignin, crude fiber, and other fluid substances, and the fibers are stuck together.²⁹ PPACC samples exhibited the presence of cobalt, which confirmed the adsorption of cobalt on the adsorbent.

Point of zero charge (PZC)

The pH dependence on the adsorption process can also be elucidated with the aid of the PZC result, which is presented in Fig. S1. PZC for PPAC was ~ 6 , which indicates that the surface charge is negative for $\text{pH} < 6$ and is positive for $\text{pH} > 6$. In the acidic pH, the surface gets protonated by OH, COOH, and NH_2 groups, while in the basic pH, those functional groups get deprotonated form and render a negative charge to the surface.²⁷ The negative outer charge of the adsorbent enhances the electrostatic attraction of the positive cobalt ion.

Effect of concentration

The impact of cobalt ion concentration on AC and RE is depicted in Fig. 3a. It was observed that the AC escalated steadily with a rise in the metal ion concentration and reached $\sim 150 \text{ mg/g}$ and the highest RE of $\sim 98 \%$ was recorded at 10 mg/L . However, the RE was found to decline continuously with a rise in the metal ion strength. An analogous trend was described in the literature for the removal of chromium ions using PP as an adsorbent.³⁰ This could be accredited to the saturation of the active sites available on the adsorbent surface with cobalt ions, which limits the removal and hence reduces the overall removal efficiency.^{30,31} As the molar ratio between the cobalt metal ion and the adsorbent active sites is moderate at a lower initial concentration, the adsorption process happens quickly.

If the molar ratio increases, the adsorption rate becomes lower, which ultimately reduces the RE i.e., leading to the exhaustion of the adsorbent active sites. Šoštarić *et al.* proposed the electrostatic repulsive force between the adsorbent and the adsorbate might also cause a decrease in the RE.³²

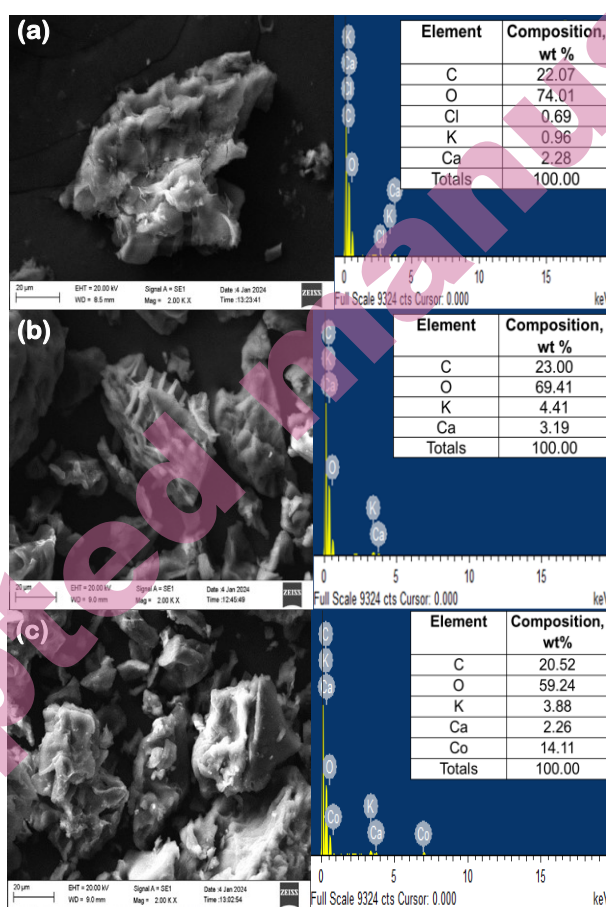


Fig. 2. SEM micrographs with EDAX analysis of (a) PP (b) PPAC and (c) PPACC.

Effect of adsorbent dose

Fig. 3b shows the impact of PPAC dose on AC and RE. Cobalt RE increases from ~55 % to ~90 % with a rise in the adsorbent dosage and then gets saturated. However, the AC decreases continuously with an escalation in the adsorbent dose. As the metal ions to the adsorbent active site ratio decreases with an increase in the dosage, the AC gets suppressed. However, the sites increase substantially with the adsorbent dose. As the active site number increases, the probability of the metal ion getting adsorbed on the surface increases, hence, the RE increases and finally

gets saturated due to the limitation of the ions in the solution.³⁰ A similar trend was also reported by Anita *et al.*, and explained the trend based on the accomplishment of the equilibrium.³³

Effect of contact time

Fig. 3c presents the influence of contact duration between the adsorbent and the cobalt metal ion on AC and RE. Both showed an increasing trend up to 90 min of contact time and then stabilized out. The AC enhanced from ~75 mg/g to ~85 mg/g with an increase in the contact duration from 15 min to 150 min. The RE increased from ~75 % to ~85 % with the contact duration from 15 min to 150 min. The adsorption of the cobalt metal ion on PPAC was found to be much faster in the initial stage and then gets saturated after the equilibrium time of 90 min is reached. The reason is that the Co(II) ions get adhered on the adsorbent surface immediately, as the active sites are more in number in the initial stages and get exhausted at the later stage.^{30,34,35}

Effect of pH

Fig. 3d elucidates the influence of pH on q_e and R using PPAC as an adsorbent. AC and RE are found to be higher on the alkaline side than on the acidic side. There is a steep rise in the value of both parameters from pH 5 to pH 9. In the lower pH, the H^+ ions compete with the adsorbate for the active sites present on the adsorbent surface. However, the cobalt ion has relatively fewer chances to occupy the active sites when compared to the H^+ ions.¹³ AC and RE tend to increase with an increase in the pH¹³ and were found to be higher near the neutral pH.³⁶ Beyond pH 8, the cobalt solution tends to precipitate out due to the formation of cobalt hydroxide.¹ This was established by the color change in the solution from pink to blue.

Effect of temperature

The influence of temperature on the AC and RE of cobalt was found to be similar in magnitude and the results are shown in Fig. 3e. AC increases continuously with the temperature from ~85 to ~89 mg g⁻¹. This dismisses the possibility of the physisorption of metal ions. Lower AC at low temperatures might be due to challenges for the diffusion of metal ions into the pores. However, at the elevated temperature due to rapid collision, the ions are forced to enter the pores of the adsorbent.^{37,38}

Adsorption isotherms

Adsorption equilibrium isotherms provide insight relationship between q_e and equilibrium concentration (C_e). The aqueous phase adsorption process may be ascertained using a range of isotherms. Langmuir, Freundlich, and Temkin isotherm models are very commonly used for adsorption studies⁶ and Eq. S-3 to S-8 (Supplementary Material) represents the linear and non-linear forms of isotherm. Langmuir adsorption is valid for homogeneous monolayer adsorption, while

Freundlich isotherm is applicable for heterogeneous multilayer adsorption.³⁹ Temkin isotherm considers the heat of adsorption of all the molecules drops steadily with adsorption. Langmuir, Freundlich, and Temkin adsorption isotherms are presented in Fig. 4 i (a-c) respectively for the linear forms and in Fig. 4 ii (a-c) for the non-linear forms. Fitting parameters of various isotherms for both linear and non-linear equations are tabulated in Table I. The best fit was obtained for the Freundlich isotherm, as the correlation coefficient value was found to be greater than the other two isotherms for both the linear and non-linear cases. This confirms that the adherence of metal ions on the adsorbent surface is heterogeneous with multilayer adsorption. Adsorption of the cobalt ion on the surface of the adsorbent is viable and favorable, as Langmuir separation factor (R_L) < 1 and $1/n < 1$ in Freundlich isotherm.

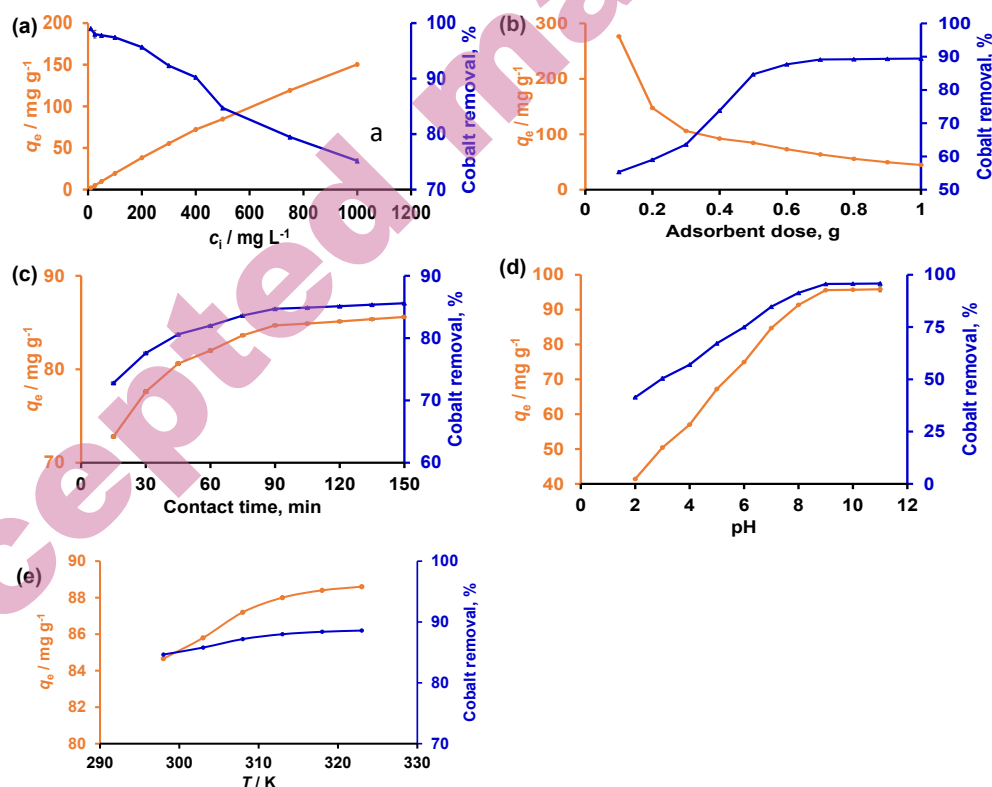


Fig. 3. Effect of (a) initial concentration (b) adsorbent dosage (c) contact duration (d) pH (e) temperature on the adsorption capacity (q_e) and cobalt ion removal efficiency using PPAC, C_i - 10 to 1000mg/L, pH - 2 to 11, time - 15 to 150 min, $T = 298 - 328$ K, dosage - 0.1 - 1.0 g.

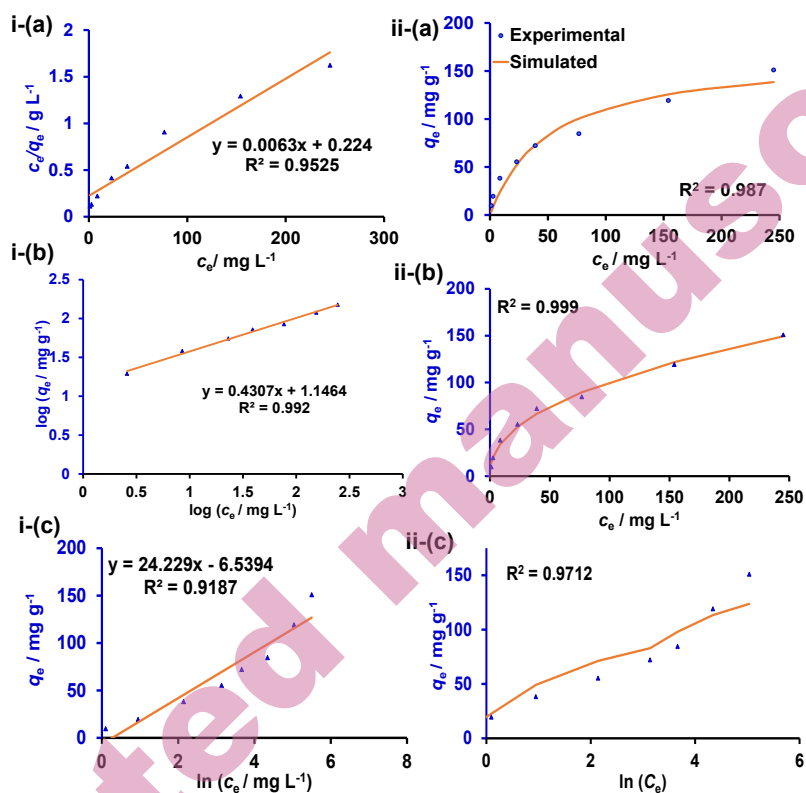


Fig. 4. (i) Linearized plot and (ii) non-linear plots of (a) Langmuir isotherm (b) Freundlich isotherm (c) Temkin adsorption isotherm models.

TABLE I. Parameters of various isotherms of Co(II) ion adsorption on PPAC.

Isotherm	Parameters	Linear	Non-linear
Langmuir	$q_m / \text{mg g}^{-1}$	158.7	100.6
	K_L / mg^{-1}	0.0285	0.0040
	R^2	0.9525	0.9871
Freundlich	K_f / g^{-1}	14.8007	8.6837
	n	2.3218	0.5011
	R^2	0.992	0.999
Temkin	$A / \text{L g}^{-1}$	86.95	0.04
	$b / \text{J g mol}^{-1} \text{mg}^{-1}$	0.0035	116.23
	R^2	0.998	0.971

Kinetic study

Kinetics studies were performed to evaluate the rate of adsorption, rate constant, order, and rate controlling step. The impact of contact duration on AC and cobalt RE data was utilized for this study. Pseudo-first order (PFO), pseudo-

second-order (PSO), and intra-particle kinetic diffusion equations are presented in Eq. S-9 to Eq. S-11 (Supplementary Material). All the models were mapped with the data and are shown in Fig. 5 (a-c). PSO model was found to be best fitted, as the correlation coefficient was found to be a higher value of 0.9998.³⁰ Kinetic fitting parameters were calculated using the slope and intercept from Fig. 5 (a-c) and are presented in Table II. The experimental and predicted value of AC is also reported in Table II. Experimental AC ($q_{e,exp}$ or q_e) is found to be comparable with the $q_{e,pred}$ for the PSO system. However, there exists a significant deviation in the adsorption values for the pseudo-first-order system. Chemisorption is the rate-limiting step, as the PSO system fits the data.⁴⁰

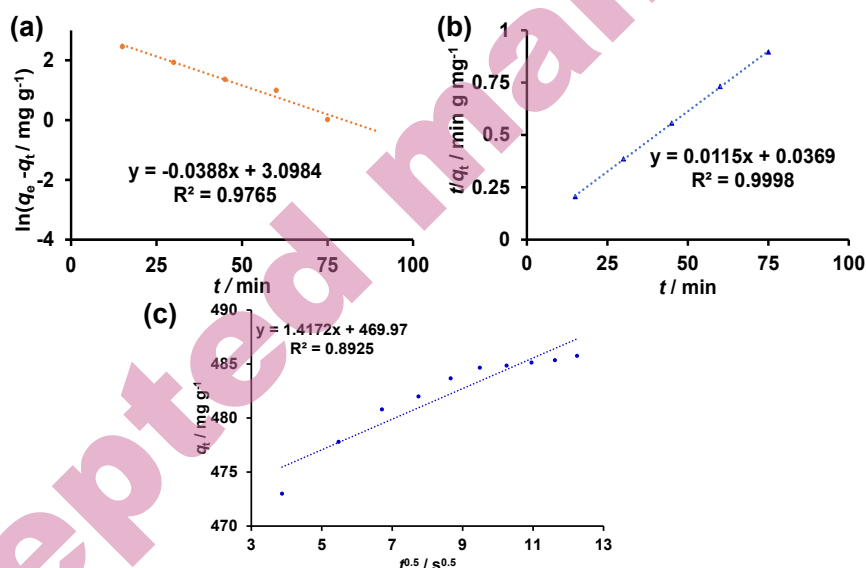


Fig. 5. Kinetics model: (a) PFO model (b) PSO model (c) intra-particle diffusion model for cobalt adsorption on PPAC.

TABLE II. Kinetic parameters of various models for Co(II) ion adsorption on PPAC.

Kinetic study	Parameter	Linear
PFO model	$q_{e,exp} / \text{mg g}^{-1}$	84.7000
	$q_{e,pred} / \text{mg g}^{-1}$	22.1600
	K_1 / min^{-1}	0.0388
	R^2	0.9765
PSO model	$q_{e,exp} / \text{mg g}^{-1}$	84.7000
	$q_{e,pred} / \text{mg g}^{-1}$	86.9500
	$K_2 / \text{g mg}^{-1} \text{min}^{-1}$	0.0035
	R^2	0.9998
Intra-particle diffusion model	$K_3 / \text{g mg}^{-1} \text{min}^{-1}$	1.4172
	R^2	0.8925

Thermodynamic parameter

Enthalpy (ΔH°) and entropy (ΔS°) were estimated from the Van't Hoff plot between $\ln(k_c)$ and $1/T$ and the plot is presented in Fig. 6. Equations used for determining the thermodynamic properties are provided in Eq. S-12 to Eq. S-14 (Supplementary Material). The positive value of (ΔH°) and (ΔS°) denotes the endothermic nature and a raise in the randomness respectively. Gibb's free energy (ΔG°) was estimated using the enthalpy and entropy values. The thermodynamic property provides a deep insight into the adsorption mechanism and the determined values are presented in Table III. A negative ΔG° value represents the spontaneity of the adsorption process.^{34,41,42}

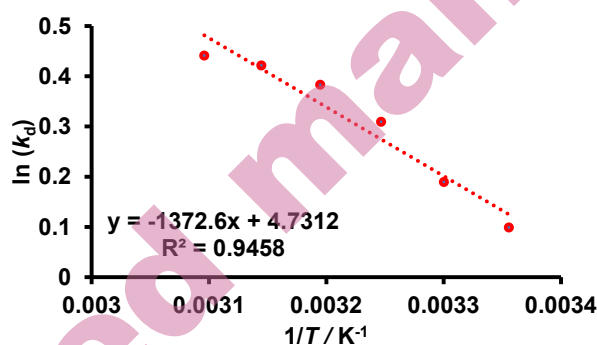


Fig. 6. Thermodynamic plot for the adsorption of Co(II) onto PPAC.

TABLE III. Thermodynamics parameter for cobalt ion adsorption on PPAC at different temperatures.

$C_i /$ mg L^{-1}	$\Delta H^\circ /$ kJ mol^{-1}	$\Delta S^\circ /$ $\text{J mol}^{-1} \text{K}^{-1}$	$\Delta G^\circ / \text{kJ mol}^{-1}$					
			298 K	303 K	308 K	313 K	318 K	323 K
500	11.42	39	-0.31	-0.51	-0.71	-0.91	-1.0	-1.30

Comparative study

The AC of PPAC towards the cobalt ion is assessed with the various adsorbents stated in the literature and the summary is presented in Table IV. PPAC showed a higher AC of 85 mg g^{-1} in comparison with most of the adsorbents reported in the literature. The proposed adsorbent follows pseudo-2nd order kinetics, Freundlich isotherm and the adsorption process is endothermic in nature. Kinetic study results reported in the present work match well with the other adsorbents utilized in the literature.^{1,6,7,9,10,11,12,38} While most of the literature reported the Langmuir adsorption isotherm, however few literatures have reported Freundlich and Dubinin-Radushkevich (D-R) model. Unlike the chemical activation or thermochemical activation process, the thermal activation process is

less expensive. The yield obtained in this study was ~55 %, which may be limitation of this study, as the continuous column study requires more adsorbent.

TABLE IV. Assessment of adsorption capacity of various adsorbents specified in the literature and the pomegranate peel.

Adsorbent	$q_e / \text{mg g}^{-1}$	Activation meth. ^a	Kinetic study ^b	Process ^c	Isotherm ^d	Ref.
Activated carbon hazel nut	13.88	TC	2 nd	Endo	L	1
Orange peel	5.128	C	2 nd	Exo	L	6
Activated carbon	51	TC	2 nd	Endo	L	7
Lemon peel	22	T	2 nd	Exo	L	9
Black tea waste	13.77	TC	1 st	-	L	10
Rice husk	35	TC	2 nd	-	L	11
Eucalyptus	55.5	C	2 nd	-	L	12
Rice husk	123	TC	2 nd	Endo	D-R	42
Mesoporous carbon	1.59	TC	2 nd	Exo	F	44
Macroalgae <i>Padina pavonica</i>	17.98	C	2 nd	Exo	L	45
Ca(OH) ₂ modified quartz rock particles	47.112	C	2 nd	Exo	L	16
Sodium borohydride	26.29	C	2 nd	Exo	L	15
Pomegranate peel	85	T	2 nd	Endo	F	This study

^aTC – Thermochemical; C – Chemical; T – Thermal

^b1st - Pseudo 1st order; 2nd - Pseudo 2nd order

^cExo – Exothermic; Endo - Endothermic

^dL – Langmuir; D-R - D-R model, F - Freundlich

CONCLUSIONS

Co(II) metal ions from simulated semiconductor industry wastewater were removed by adsorption on PPAC. Several factors *viz.*, inceptive metal ion concentration, temperature, dosage, pH, and contact duration were varied to determine their effect on the AC. Adsorption of Co(II) ions on PPAC shadowed PSO kinetics. Freundlich isotherm fitted well for the adsorption data with linear/non-linear correlation coefficient of 0.992 / 0.99 respectively. Maximum cobalt ion adsorption of ~85 mg g⁻¹ was obtained at neutral pH without the formation of cobalt hydroxides. The evaluation of thermodynamic parameters for PPAC demonstrated that the adsorption of Co(II) ions was endothermic with a positive value of ΔH° , whereas the rise in degree of spontaneity is confirmed by a negative value of ΔG° and increase in disorder of the adsorption process is indicated by the positive value of ΔS° . PPAC, a low-cost adsorbent from agricultural waste, is proven for the exclusion of Co(II) ions from wastewater. The

preparation of proposed adsorbent is simpler, cheaper and environmentally benign, as the pomegranate peel, thrown as waste material, was utilized. The desorption study of the spent PPACC *i.e.*, regeneration of adsorbent can be considered as future research.

SUPPLEMENTARY MATERIAL

Additional data are available electronically at the pages of journal website: <https://www.shd-pub.org.rs/index.php/JSCS/article/view/12983>, or from the corresponding author on request.

ИЗВОД

БИОСОРПТИВНО УКЛАЊАЊЕ ЈОНА КОБАЛТА (II) ИЗ ОТПАДНИХ ВОДА КОРИШЋЕЊЕМ АКТИВНОГ УГЉА ОД КОРЕ НАРА КАО БИОСОРБЕНТА

SUSHMA, AMIT KESHAV, MANIVANNAN RAMACHANDRAN

Department of Chemical Engineering, National Institute of Technology Raipur, Chhattisgarh, India.

Кобалт се користи за повезивање компоненти током производње интегрисаних кола (IC). Јони кобалта се уобичајено налазе у истрошеној суспензији хемијско механичке планаризације (СМР). Улога кобалта (Co) је незаменљива у индустрији полупроводника и његово присуство у отпадним водама је неизбежно. Јони кобалта су токсични и могу изазвати озбиљне здравствене проблеме као што су болести срца, мучнина, оштећење вида, оштећење штитне жлезде, дефекте костију и дијареју. Овај рад истражује потенцијалну примену активног угља добијеног од *Punica granatum* (нар) (PPAC) као адсорбента за уклањање јона кобалта. У овом раду се испитује утицај почетне концентрације јона кобалта, рН, трајање контакта и доза адсорбента на ефикасност уклањања (RE) и адсорпциони капацитет (AC) јона Co^{2+} , и разматрају нађени резултати. Кинетичка студија адсорпције Co(II) показала је да се псеудо-други ред најбоље уклапа са константом брзине од $\sim 0.00358 \text{ g mg}^{-1} \text{ min}^{-1}$. Адсорбент који је коришћен у овом раду је процењен помоћу SEM, EDAX, FTIR, XRD и TGA. EDX састав узорка након адсорпције показао је присуство кобалта. Адсорпција јона кобалта на PPAC најбоље одговара моделу Freundlich изотерме. Утврђено је да је адсорпција Co(II) ендотермна на основу термодинамичких карактеристика процењених за угљеник. На температури спољашње средине ($\sim 303 \text{ K}$) и неутралном рН, утврђено је да PPAC има максималну AC од $\sim 85 \text{ mg/g}$, са RE од $\sim 90 \%$.

(Примљено 20. маја; ревидирано 13. јуна; прихваћено 27. септембра 2024.)

REFERENCES

1. E. Demirbaş, *Adsorpt. Sci. Technol.* **21** (2003) 951 (<https://doi.org/10.1260/02636170360744380>)
2. F. S. Khoo, H. Esmacili, *J. Serb. Chem. Soc.* **83** (2018) 237 (<https://doi.org/10.2298/JSCJSC170704098S>)
3. B. Ma, S. Zhang, B. Tan, W. Li, Y. Wang, X. Sun, *Colloids Surf. A: Physicochem. Eng. Asp.* **652** (2022) 129816 (<https://doi.org/10.1016/j.colsurfa.2022.129816>)
4. H. N. M. E. Mahmud, A. K. O. Huq, R.B. Yahya, *R. Soc. Chem. Adv.* **6** (2016) 14778 (<https://doi.org/10.1039/C5RA24358K>)

5. M. H. Salmani, M. H. Ehrampoush, H. Eslami, B. Eftekhar, *Groundw. Sustain. Dev.* **11** (2020) 100425 (<https://doi.org/10.1016/j.gsd.2020.100425>)
6. Y. Altunkayank, M. Canpolat, Ö. Yavuz, *J. Iran. Chem. Soc.* **6** (2022) 2437 (<https://doi.org/10.1007/s13738-021-02458-8>)
7. B. Kakavandi, R. Raofi, S. M. Peyghambarzadeh, B. Ramavandi, M. H. Niri, M. Ahmadi, *Desalin. Water Treat.* **111** (2018) 310 (<https://doi.org/10.5004/dwt.2018.22238>)
8. A. A. Babaei, S. N Alavi, M. Akbarifar, K. Ahmadi, A. R. Esfahai, B. Kakavandi, *Desalin. Water Treat.* **57** (2016) 27199 (<https://doi.org/10.1080/19443994.2016.1163736>)
9. A. Bhatnagar, A. K. Minocha, M. Sillanpää, *Biochemi. Eng. J.* **48** (2010) 181 (<https://doi.org/10.1016/j.bej.2009.10.005>)
10. R. R. Mohammed, *Arab. J. Sci. Eng.* **37** (2012) 1505 (<https://doi.org/10.1007/s13369-012-0264-8>)
11. D. S. P. Franco, J. M. Cunha, G. F. Dortzbacher, G. L. Dotto, *Process Saf. Environ. Prot.* **109** (2017) 55 (<https://doi.org/10.1016/j.psep.2017.03.029>)
12. Y. Essaadaoui, A. Lebkiri, E. Rifi, L. Kadiri, A. Ouas, *Mediterr. J. Chem.* **7** (2018) 145 (<http://doi.org/10.13171/mjc72/01808150945-essaadaoui>)
13. S. Ben-Ali, I. Jaouali, S. S. Najjar, *J. Clean. Prod.* **142** (2017) 3809 (<https://doi.org/10.1016/j.jclepro.2016.10.081>)
14. W. Saadi, S. Rodríguez-Sánchez, B. Ruiz, S. Najjar-Souissi, A. Ouederni, E. Fuente *J. Environ. Chem. Eng.* **10** (2022) 107010 (<https://doi.org/10.1016/j.jece.2021.107010>)
15. H. S. Kalal, H. Rashedi, Z. S. Yekta, M. Taghiof, *Microporous Mesoporous Mater.* **366** (2024) 119244 (<https://doi.org/10.1016/j.micromeso.2023.112944>)
16. F. A. Rasheed, M. Sillanpää, M. Marodi, *Desalin. Water Treat.* **319** (2024) 100477 (<https://doi.org/10.1016/j.dwt.2024.100477>)
17. A. Hashem, C. O. Aniagor, M. Fikry, G. M. Taha, S. M. Badawy, *J. Mater. Cycles Waste Manag.* **25** (2023) 2087 (<https://doi.org/10.1007/s10163-023-01655-2>)
18. S. Hemmalakshmi, S. Priyanga, K. Devaki, *J. Pharm. Sci. Res.* **9** (2017) 2062 (<https://www.jpsr.pharmainfo.in/Documents/Volumes/vol9Issue11/jpsr09111718.pdf>)
19. O. F. Vázquez-Vuelvas, F. A. Chávez-Camacho, J. A. Meza-Velázquez, E. Mendez-Merino, M. M. Ríos-Licea, J. C. Contreras-Esquivel, *Food Hydrocoll.* **103** (2020) 105642 (<https://doi.org/10.1016/j.foodhyd.2020.105642>)
20. K. Yang, H. Peng, Y. Wen, N. Li, *Appl. Surf. Sci.* **256** (2010) 3093 (<https://doi.org/10.1016/j.apsusc.2009.11.079>)
21. P. P. Satapute, B. N. Patil, B. B. Kaliwal, *Int. J. Sci. Res. Rev.* **6** (2017) 49 (<https://www.ijrr.org/pdf/619.pdf>)
22. J. O. Loza, F. Chejne, A. G. A. Jameel, S. Telalovic, A. A. Arrieta, S. M. Sarathy, *J. Environ. Chem. Eng.* **9** (2021) 106144 (<https://doi.org/10.1016/j.jece.2021.106144>)
23. F. D'Amico, M. E. Musso, R. J. F. Berger, N. Cefarin, G. Birarda, G. Tondi, D. B. Menezes, A. Reyer, L. Scarabattoli, T. Sepperer, T. Schnabel, L. Vaccari, *Spectrochim. Acta A. Mol. Biomol. Spectrosc.* **262** (2021) 120090 (<https://doi.org/10.1016/j.saa.2021.120090>)
24. L. Yuzhen, D. Changwen, S. Yanqiu, Z. Jianmin, *J. Food Sci. Eng.* **4** (2014) 244 (<https://www.davidpublisher.com/Public/uploads/Contribute/552cb6304219e.pdf>)

25. M. Indhumathi, A. Arunprasath, *J. Drug Deliv. Ther.* **9** (2019) 583 (<http://dx.doi.org/10.22270/jddt.v9i3-s.3003>)
26. Ş. Altındal, Ö. Sevgili, Y. Azizian-Kalandaragh, *J. Mater. Sci.: Mater. Electron.* **30** (2019) 9273 (<https://doi.org/10.1007/s10854-019-01257-5>).
27. I. Akkari, Z. Graba, N. Bezzi, M. Vithanage, M. M. Kaci, *Biomass Conv. Bioref.* **14** (2022) 1 (<https://doi.org/10.1007/s13399-022-03401-4>)
28. I. Akkari, Z. Graba, N. Bezzi, F. A. Merzeg, N. Bait, A. Ferhati, *Biomass Conv. Bioref.* **13** (2023) 8047 (<https://doi.org/10.1007/s13399-021-01620-9>)
29. E.A. Abdel-Galil, L. Hussin, W. El-Kenany, *Desalin. Water Treat.* **211** (2021) 250 (<https://doi.org/10.5004/dwt.2021.26588>)
30. R. Giri, N. Kumari, M. Behera, A. Sharma, S. Kumar, N. Kumar, R. Singh *Environmental Sustainability* **4** (2021) 401 (<https://doi.org/10.1007/s42398-021-00192-8>)
31. T. A. H. Nguyen, W. S. Guo, J. Zhang, S. Liang, Q. Y. Yue, Q. Li, T. V. Nguyen, *Bioresour. Technol.* **148** (2013) 574 (<https://doi.org/10.1016/j.biortech.2013.08.124>)
32. T. D. Šoštarić, M. S. Petrović, F. T. Pastor, D. R. Lončarević, J. T. Petrović, J. V. Milojković, M. D. Stojanović, *J. Mol. Liq.* **259** (2018) 340 (<https://doi.org/10.1016/j.molliq.2018.03.055>)
33. D. Anitha, A. Ramadevi, R. Seetharaman, *Mater. Today: Proc.* **45** (2021) 718 (<https://doi.org/10.1016/j.matpr.2020.02.748>)
34. T. S. Badessa, E. Wakuma, A. M. Yimer, *BMC Chem.* **14** (2020) 71 (<https://doi.org/10.1186/s13065-020-00724-z>)
35. R. Garg, R. Garg, M. Sillanpää, Alimuddin, M. A. Khan, N. M. Mubarak, Y. H. Tan, *Sci. Rep.* **13**(2023) 6859 (<https://doi.org/10.1038/s41598-023-33843-3>)
36. M. Abbas, S. Kaddour, M. Trari, *J. Ind. Eng. Chem.* **20** (2014) 745 (<https://doi.org/10.1016/j.jiec.2013.06.030>)
37. L. Panda, S. K. Jena, S. S. Rath, P. K. Misra, *Environ. Sci. Pollut. Res.* **27** (2020) 24284 (<https://doi.org/10.1007/s11356-020-08482-0>)
38. K. Yetilmmezsoy, D. Özçimen, A. T. Koçer, M. Bahramian, E. Kıryan, H. M. Akbin, B. Goncaloğlu, *Int. J. Environ. Res.* **14** (2020) 541 (<https://doi.org/10.1007/s41742-020-00275-0>)
39. A. O. Dada, A. P. Olalekan, A. M. Olatunya, O. Dada, *IOSR J. Appl. Chem.* **3** (2012) 38 (<https://www.iosrjournals.org/iosr-jac/papers/vol3-issue1/J0313845.pdf>)
40. M. Nasser, M. Abbas, M. Trari, *Prog. React. Kinet. Mec.* **49** (2024) 14686783241226858. (<https://doi.org/10.1177/14686783241226858>)
41. G. Dönmez, Z. Aksu, *Process Biochem.* **38** (2002) 751 ([https://doi.org/10.1016/S0032-9592\(02\)00204-2](https://doi.org/10.1016/S0032-9592(02)00204-2))
42. H. Nadaroglu, E. Kalkan, *Int. J. Phys. Sci.* **7** (2012) 1386 (<https://doi.org/10.5897/IJPS11.1748>)
43. H. M. H. Gad, H. A. Omar, M. Aziz, M. R. Hassan, M. H. Khalil, *Asian J. Chem.* **28** (2016) 385 (<http://dx.doi.org/10.14233/ajchem.2016.19364>)
44. M. N. Siddiqui, B. Chanbsha, A. A. Alfraj, T. K. Kova, I. Ali, (<https://doi.org/10.1016/j.eti.2020.101257>)
45. A. S. Aloufi, B. A. Riyami, M. A. Fawzy, H. M. Al-Yasi, M. Koutb, S. H. A. Hassan, *Water* **16** (2024) 887 (<https://doi.org/10.3390/w16060887>).